# Electronic Supplementary Information

## A chiral BINOL-based supramolecular gel enabling sensitive enantioselective and chemoselective collapse toward histidine

Yixuan Jiang,[a] Zeng Huang,[b] Jun Tian,[a] Xin Dong,[a] Xiao-Qi Yu [a,c] and Shanshan Yu *[a]

[a] *Key Laboratory of Green Chemistry and Technology, Ministry of Education, College of Chemistry, Sichuan University, Chengdu 610064, China*

[b] *Institute of Nuclear Physics and Chemistry, China Academy of Engineering Physics, Mianyang 621900, China*

[c] *Asymmetric Synthesis and Chiral Technology Key Laboratory of Sichuan Province, Department of Chemistry, Xihua University, Chengdu 610039, P. R. China*

*Corresponding author e-mail: yushanshan@scu.edu.cn (S.Yu).

# Table of Contents

## 1. Experimental Procedures

### 1.1 Materials

Unless otherwise noted, materials were obtained from commercial suppliers and used without further purification. All solvents for the optical spectroscopic studies were either high-performance liquid chromatography- or spectroscopic-grade.

### 1.2 Characterization Methods

A Bruker Avance II-400 MHz NMR spectrometer were used for NMR analysis, and a Bruker Avance II-600 MHz NMR spectrometer was used for temperature-dependent $^{1}$H NMR analysis. HRMS spectra were measured on a Bruker Daltonics Bio TOF mass spectrometer. Fluorescence spectra were collected on a Hitachi F-7000 fluorescence spectrophotometer. Circular dichroism (CD) spectra and UV-Vis absorption spectra were measured with Applied Photophysics Chirascan. The dilute solution ($1\times10^{-4}$ M) were placed in quartz cuvettes (light path 1 mm), while the others were placed in quartz cuvettes (light path 0.1 mm). Circularly polarized luminescence (CPL) spectra were performed on a JASCO CPL-300 spectrofluoropolarimeter. The FT-IR (KBr pellet) spectra were recorded (400-4000 $cm^{-1}$ region) on a Nicolet Impact 410 FT-IR spectrometer. Scanning Electron Microscopy (SEM) images were performed on a JSM-5900LV (JEOL, Japan). Transmission electron microscopy (TEM) images were performed on a Talos F200S instrument. Rheological analyses were performed on a DHR-2 rheometer using a 40 mm parallel-plate geometry at 25 ℃. Dynamic frequency sweep experiments were carried out at a constant strain of 0.1% between 0.1-100 rad/s. Dynamic strain sweep experiments were carried out at a constant frequency of 6.28 rad/s between 0.1%-100%. The Crystal X-ray Diffraction (XRD) data was collected on a Bruker APEX-II CCD diffractometer with Mo-Kα (λ = 0.71073 Å) at 302 K.

### 1.3 Gelation Test by the Inverted Vial Method

The (*R*)-$H_3L$ (10 mg) in vials was dissolved in various solvents by heating. These samples were allowed to cooled to room temperature, and the formation of gels was confirmed by the inverted vial method. If (*R*)-$H_3L$ and solvent were fixed at the bottom of the vial and could not flow, gel was considered to be formed. In the vial where the gel was formed, a certain amount of solvent was added until the stable gel was not obtained. At this time, the concentration obtained is the CGC of (*R*)-$H_3L$ in this solution.

### 1.4 Crystal growth of (*R*)-$H_3L$

The (*R*)-$H_3L$ (3 mg) in vials was dissolved in 100 μL ethanol and 100 μL $H_2O$, slow evaporation of solvent in 40 ℃ resulted in several colorless block-shaped crystals.

**1.5 Visual chiral sensing of (*R*)-$H_3L$-Cu Gel**

To a solution of (*R*)-$H_3L$ (5 mg) in EtOH (0.30 mL), a solution of copper chloride (1.0 equiv) in water (0.20 mL) and a solution of amino acid (0.01 equiv) in water (0.10 mL) was added. The mixture was dissolved and mixed evenly by heating, and the glass vial was inverted after cooling to room temperatur to observe whether a stable gel was formed. Blank control group was added with pure water.

**2. Synthesis of (*R*)-$H_3L$**

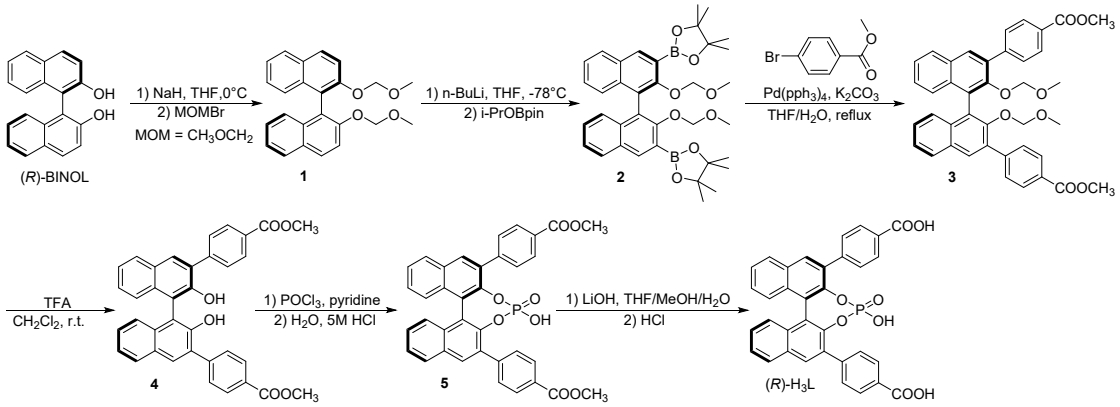


**Scheme S1.** Synthesis of (*R*)-$H_3L$

Synthesis of **1**

To a suspension of (*R*)-BINOL (20.0 g, 70 mmol) in anhydrous THF (200 mL) was added sodium hydride (11.2 g, 280 mmol, in 50 mL anhydrous THF) under ice bath. After stirring for 2 h at room temperature, bromomethyl methyl ether (18 mL, 210 mmol) was added dropwise under ice bath, and the resulting mixture was heated to room temperature and stirred for 1 h. Upon completion of the reaction monitored by TLC, the reaction mixture was quenched by saturated aqueous $NH_4Cl$ solution, extracted with $CH_2Cl_2$ (100 mL ×3), dried over $Na_2SO_4$, and concentrated under reduced pressure. The crude product was purified by recrystallizing from methanol to afford **1** (26.0 g) as a white crystal in 99% yield. $^1$H NMR (400 MHz, Chloroform-*d*) δ 7.94 (d, *J* = 9.1 Hz, 2H), 7.86 (d, *J* = 8.2 Hz, 2H), 7.57 (d, *J* = 9.0 Hz, 2H), 7.36 – 7.31 (m, 2H), 7.21 (t, *J* = 7.6 Hz, 2H), 7.15 (d, *J* = 8.5 Hz, 2H), 5.08 (d, *J* = 6.8 Hz, 2H), 4.97 (d, *J* = 6.8 Hz, 2H), 3.13 (s, 6H). $^{13}$C NMR (101 MHz, Chloroform-*d*) δ 152.8,

134.1, 130.0, 129.5, 128.0, 126.4, 125.7, 124.2, 121.4, 117.4, 95.3, 56.0. HR-MS ($ES^+$) calculated for $C_{24}H_{22}O_4Na^+$ ($M+Na^+$) 397.1410, found 397.1390.

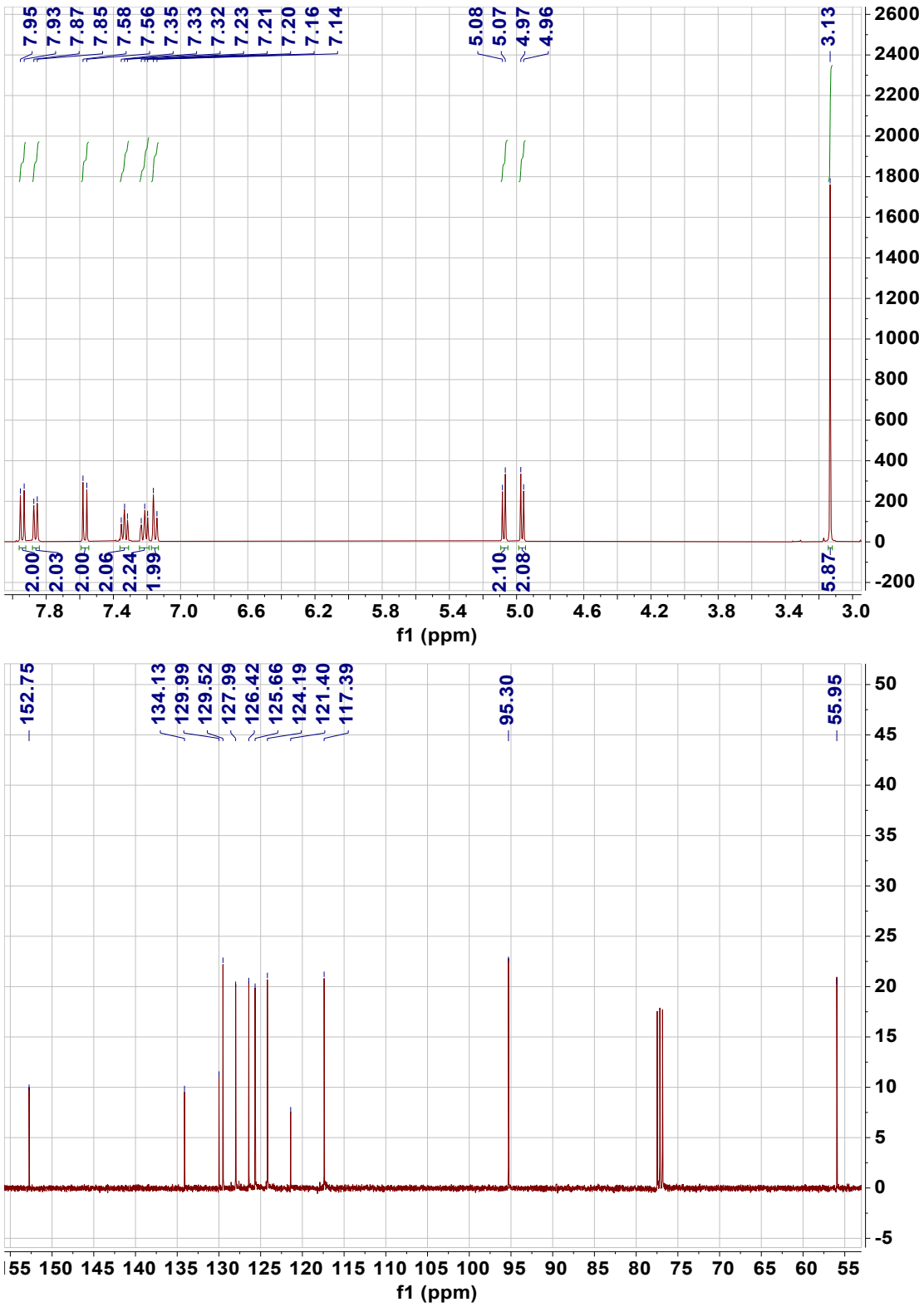


**Figure S1.** $^1H$ NMR (400 MHz, Chloroform-*d*) and $^{13}C$ NMR (101 MHz, Chloroform-*d*) spectra of **1**.

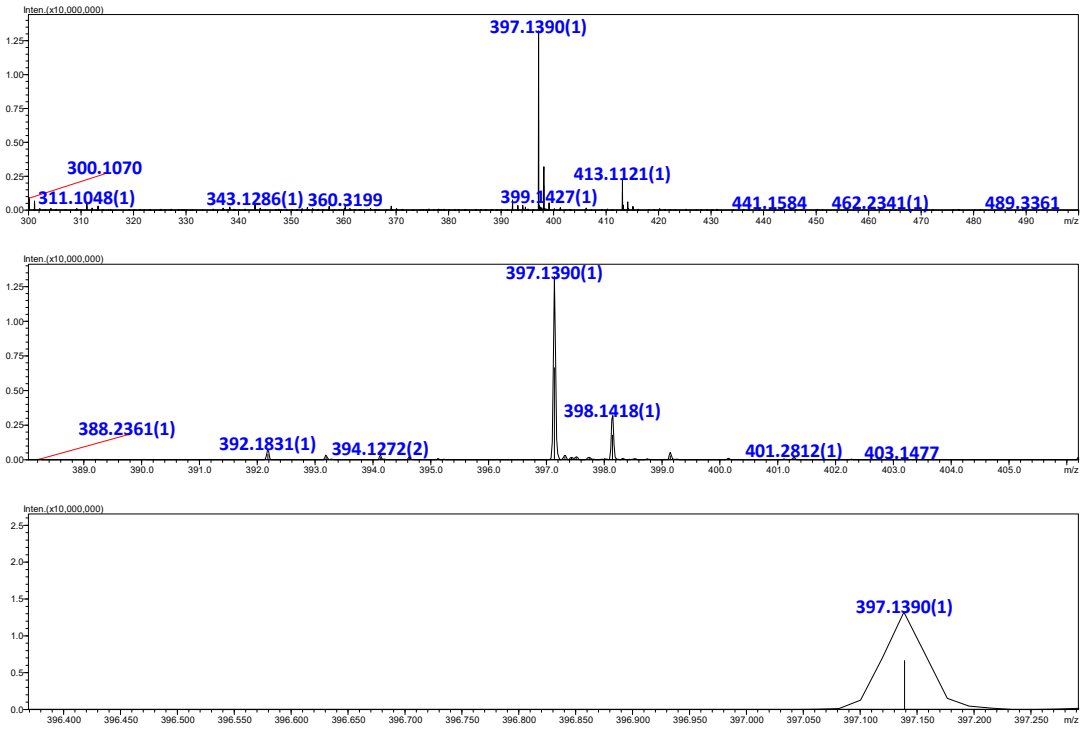


**Figure S2.** HRMS spectra of **1** ($ES^+$).

Synthesis of **2**

To a suspension of **1** in anhydrous THF (250 mL) was slowly added *n*-BuLi (25 mL, 62.5 mmol, 2.5 M in hexane) over 15 min at -78°C. After stirring for 7 h at room temperature, the resulting mixture was cooled to -78°C, and *i*-PrOBpin (13 mL, 62.5 mmol) was added over 10 min. The solution was warmed to room temperature and stirred for 12 hours. Upon completion of the reaction monitored by TLC, the reaction mixture was quenched by saturated aqueous $NH_4Cl$ solution, extracted with EtOAc (100 mL ×3), the combined organic layer was washed with brine (100 mL), dried over $Na_2SO_4$, and concentrated under reduced pressure. The crude product was purified by silica gel column chromatography eluting with hexane/EtOAc to give **2** (8.0 g) as a white powder in 51% yield. $^1H$ NMR (400 MHz, Chloroform-*d*) δ 8.44 (s, 2H), 7.88 (d, $J$ = 8.2 Hz, 2H), 7.35 (t, $J$ = 6.9 Hz, 2H), 7.23 (d, $J$ = 8.6 Hz, 2H), 7.17 (d, $J$ = 8.4 Hz, 2H), 4.89 – 4.82 (m, 4H), 2.25 (s, 6H), 1.36 (s, 24H). $^{13}C$ NMR (101 MHz, Chloroform-*d*) δ 157.2, 139.3, 136.2, 130.3, 128.4, 127.3, 126.9, 126.0, 124.7, 100.1, 84.0, 55.6, 25.0, 25.0. HR-MS ($ES^+$) calculated for $C_{36}H_{44}B_2O_8Na^+$ ($M+Na^+$) 649.3115, found 649.3100.

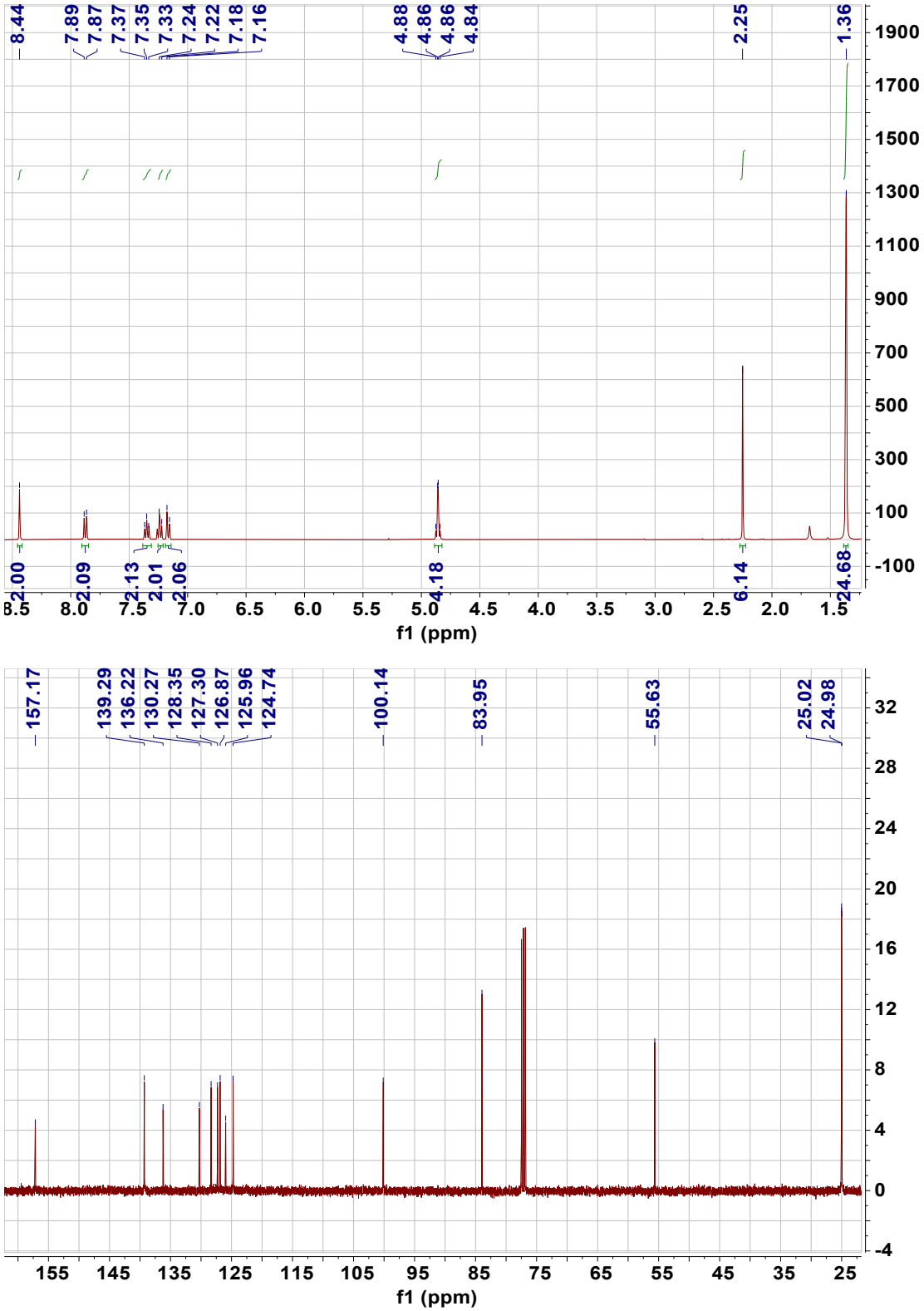


**Figure S3.** $^{1}$H NMR (400 MHz, Chloroform-*d*) and $^{13}$C NMR (101 MHz, Chloroform-*d*) spectra of **2**.

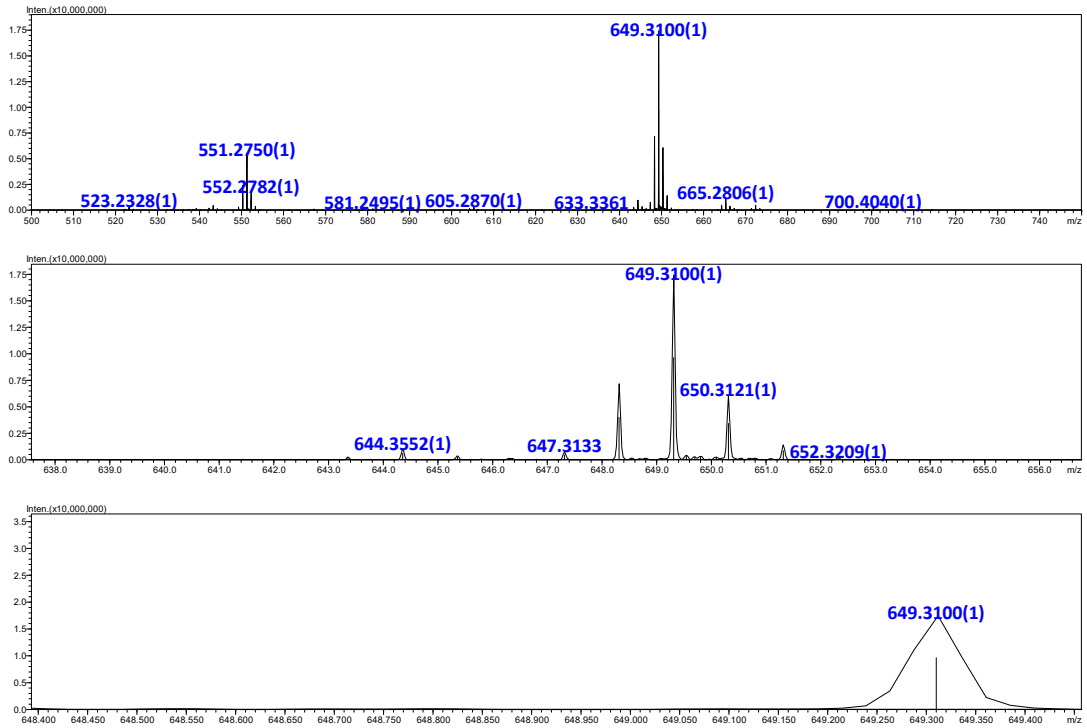


**Figure S4.** HRMS spectra of **2** ($ES^+$).

Synthesis of **3**

A 500 mL flame-dried round-bottom flask was charged with **2** (10.0 g, 16 mmol), methyl 4-bromobenzoate (8.6 g, 40 mmol) and tetrakis triphenylphosphine palladium (1.85 g, 1.6 mmol), degassed and refilled with argon for three times. Then degassed THF (200 mL) and 2 M $K_2CO_3$ solution (30 mL, aq.) was added, and the suspension was heated under reflux conditions for 24 hours. After cooling to room temperature, the resulting mixture was filtered with diatomite, extracted with $CH_2Cl_2$ (100 mL ×3), dried over $Na_2SO_4$, and concentrated under reduced pressure. The crude product was purified by silica gel column chromatography eluting with hexane/$CH_2Cl_2$ to afford **3** (8.2 g) as a light yellow solid in 80% yield. $^1$H NMR (400 MHz, Chloroform-*d*) δ 8.15 (d, *J* = 7.5 Hz, 4H), 7.98 (s, 2H), 7.91 (d, *J* = 8.9 Hz, 2H), 7.85 (d, *J* = 7.5 Hz, 4H), 7.44 (t, *J* = 7.3 Hz, 2H), 7.30 (q, *J* = 8.6 Hz, 4H), 4.41 – 4.33 (m, 4H), 3.96 (s, 6H), 2.35 (s, 6H). $^{13}$C NMR (101 MHz, Chloroform-*d*) δ 167.0, 151.1, 143.7, 134.4, 133.8, 130.8, 130.7, 129.7, 129.6, 128.9, 128.0, 126.8, 126.5, 126.3, 125.4, 98.0, 56.0, 52.2. HR-MS ($ES^+$) calculated for $C_{40}H_{35}O_8^+$ ($M+H^+$) 665.2146, found 665.2121.

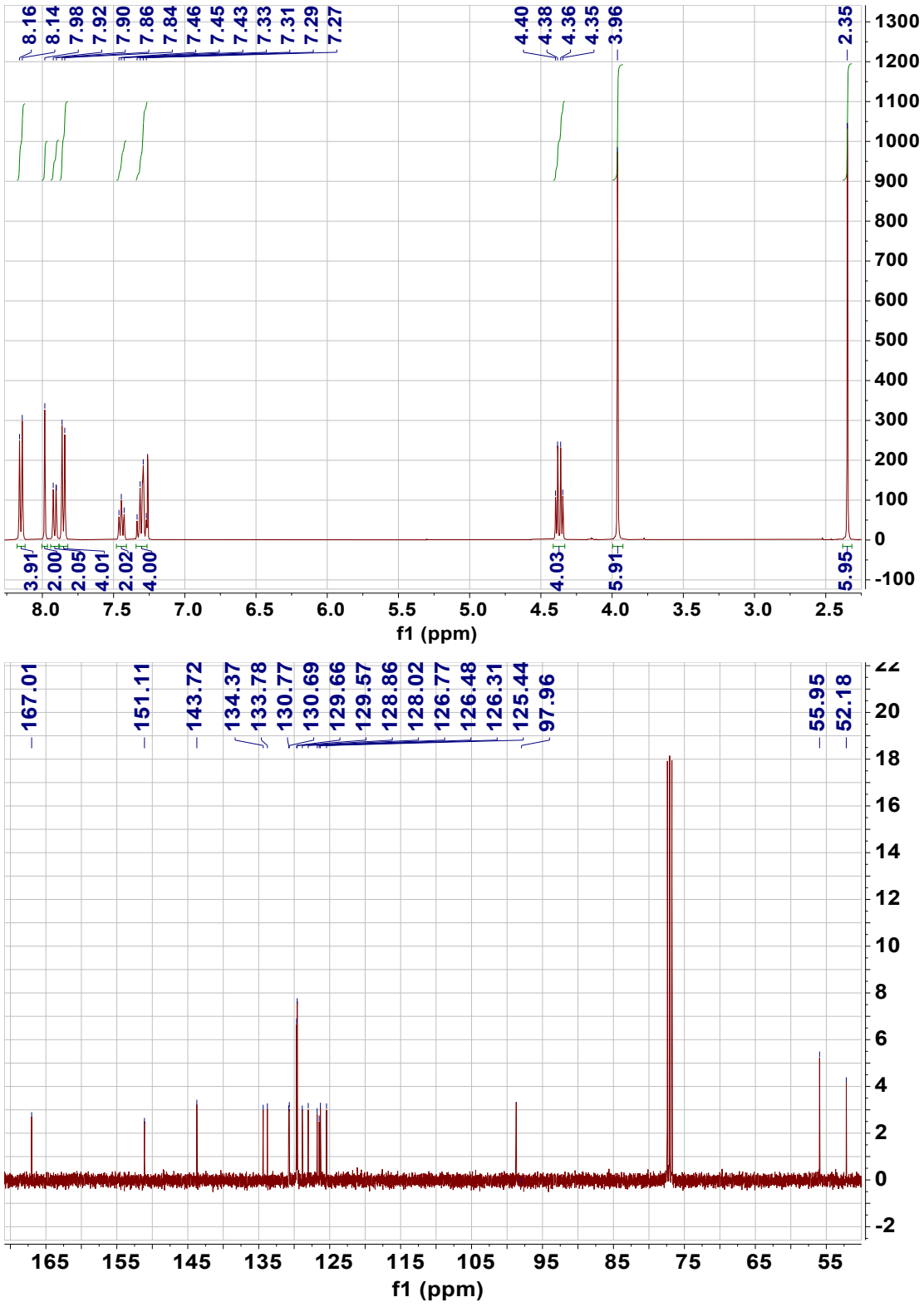


**Figure S5.** $^{1}$H NMR (400 MHz, Chloroform-*d*) and $^{13}$C NMR (101 MHz, Chloroform-*d*) spectra of **3**.

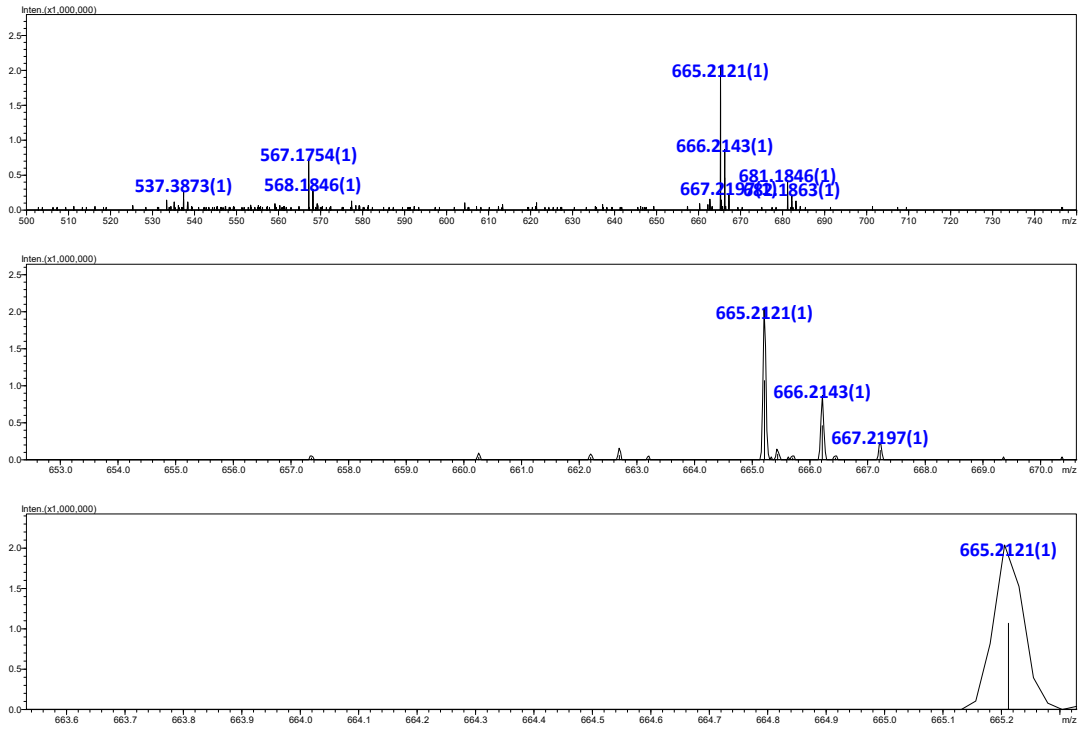


**Figure S6.** HRMS spectra of **3** ($ES^+$).

Synthesis of **4**

To a solution of **3** ( 8.2 g, 12.8 mmol) in $CH_2Cl_2$ (200 mL) was added trifluoroacetic acid (20 mL). After stirring at room temperature for 8 h, the reaction mixture was quenched by saturated aqueous sodium bicarbonate solution, extracted with $CH_2Cl_2$ (100 mL ×3), dried over $Na_2SO_4$, and concentrated under reduced pressure. The crude product was dissolved in a small amount of $CH_2Cl_2$ and a large amount of hexane, stirred at room temperature overnight and filtered to give **4** (6.2 g) as a light orange solid in 90% yield.$^1$H NMR (400 MHz, Chloroform-*d*) δ 8.28 – 8.05 (m, 6H), 7.89 (dd, *J* = 47.9, 8.4 Hz, 6H), 7.52 – 7.32 (m, 4H), 7.22 (d, *J* = 8.3 Hz, 2H), 3.94 (s, 6H). $^{13}$C NMR (101 MHz, Chloroform-*d*) δ 167.2, 150.3, 142.4, 133.2, 132.0, 129.8, 129.7, 129.5, 129.3, 128.8, 128.1, 125.4, 124.3, 52.4. HR-MS ($ES^+$) calculated for $C_{36}H_{27}O_6^+$ ($M+H^+$) 555.1802, found 555.1801.

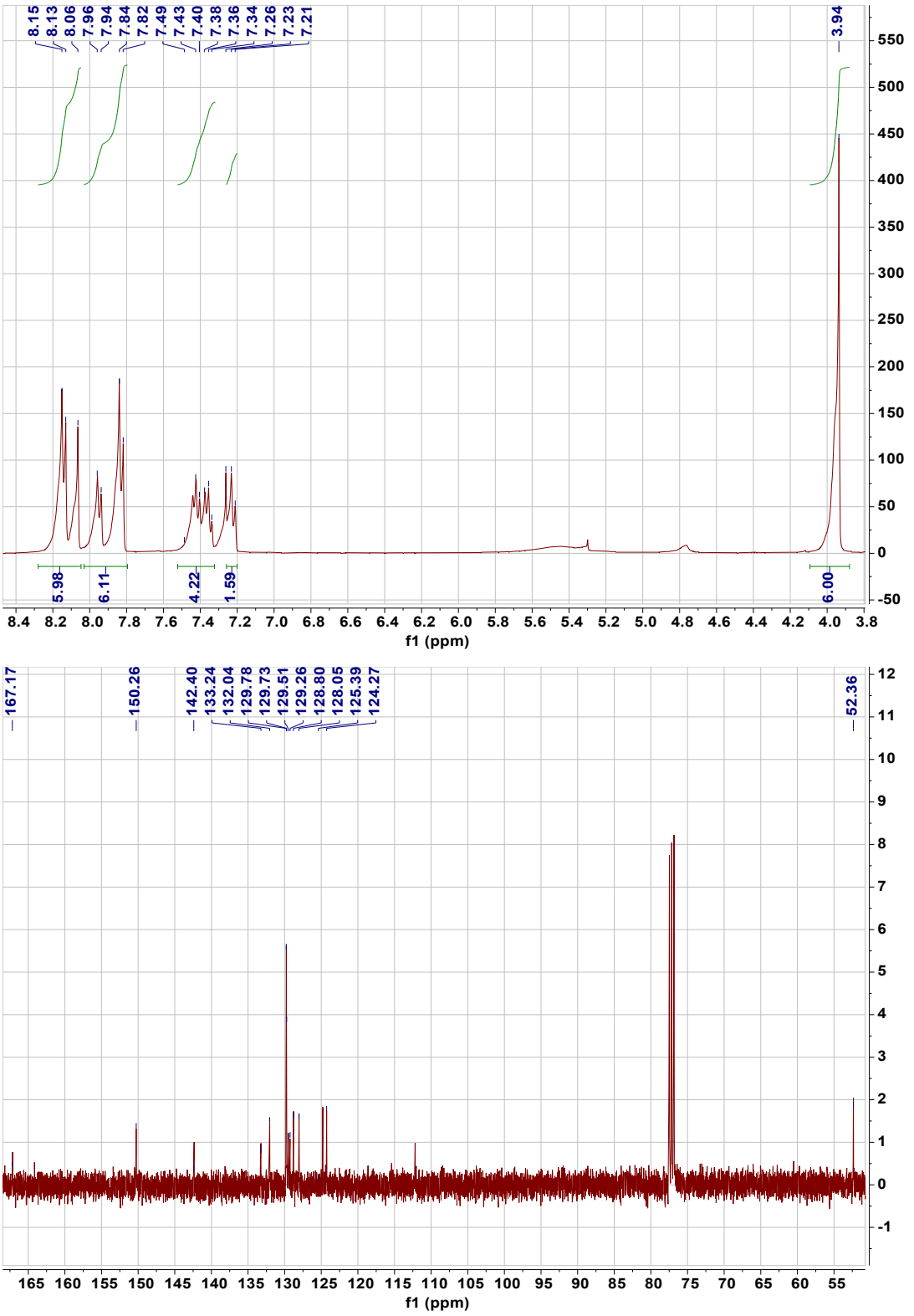


**Figure S7.** $^{1}$H NMR (400 MHz, Chloroform-*d*) and $^{13}$C NMR (101 MHz, Chloroform-*d*) spectra of **4**.

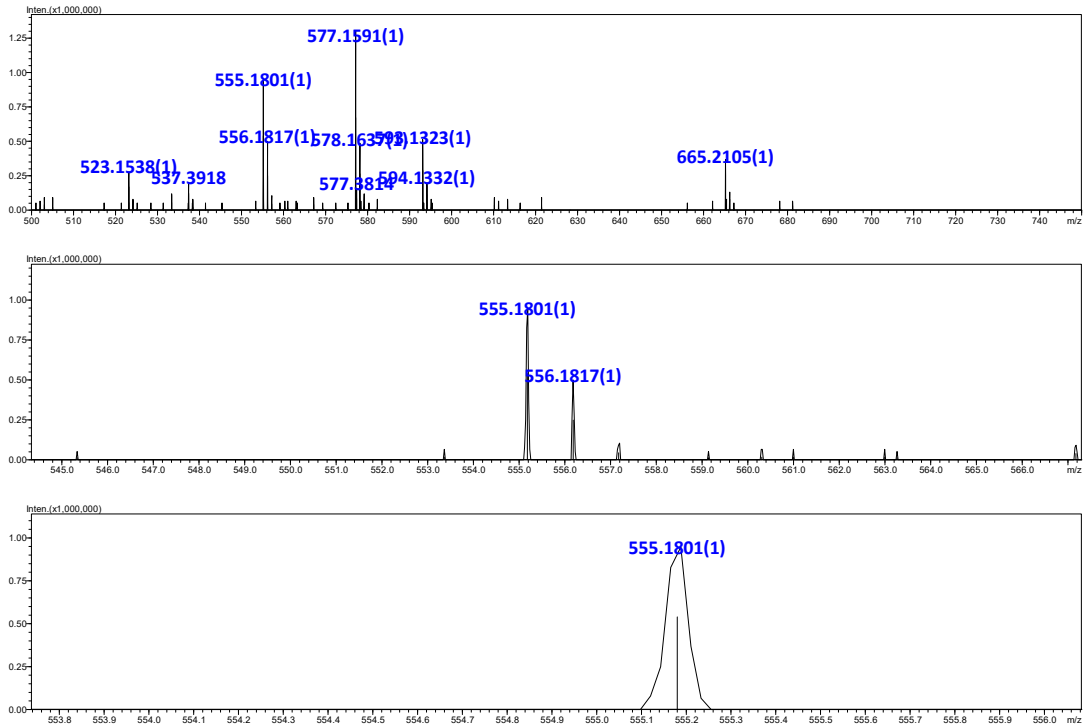


**Figure S8.** HRMS spectra of **4** ($ES^+$).

Synthesis of **5**

To a solution of **4** (0.22 g, 0.4 mmol) in anhydrous pyridine (1 mL) was added phosphorus oxychloride (0.15 mL, 1.6 mmol). After stirring at room temperature for 3 h, the reaction mixture was quenched by water, and stirred for additional 20 min. After evaporation of pyridine under vacuum, 5M HCl (1 mL, aq.) was added to the residue. The reaction mixture was stirred at room temperature for 1 h, then filtered and washed with water to give the crude product. The crude product was purified by silica gel column chromatography eluting with EtOAc/methanol to give **5** (0.2 g) as a white powder in 80% yield. $^1$H NMR (400 MHz, DMSO-$d_6$) δ 8.18 (d, $J$ = 8.5 Hz, 6H), 8.09 (d, $J$ = 8.2 Hz, 2H), 8.05 (d, $J$ = 8.2 Hz, 4H), 7.47 (t, $J$ = 7.5 Hz, 2H), 7.31 (t, $J$ = 7.7 Hz, 2H), 7.08 (d, $J$ = 8.5 Hz, 2H), 3.90 (s, 6H). $^{13}$C NMR (101 MHz, DMSO-$d_6$) δ 166.3, 142.9, 133.2, 132.1, 130.6, 130.1, 128.8, 128.7, 128.2, 126.7, 126.6, 126.0, 125.1, 122.7, 52.2. $^{31}$P NMR (162 MHz, DMSO-$d_6$) δ 2.90. HR-MS ($ES^+$) calculated for $C_{36}H_{26}O_8P^+$ ($M+H^+$) 639.1179, found 639.1175.

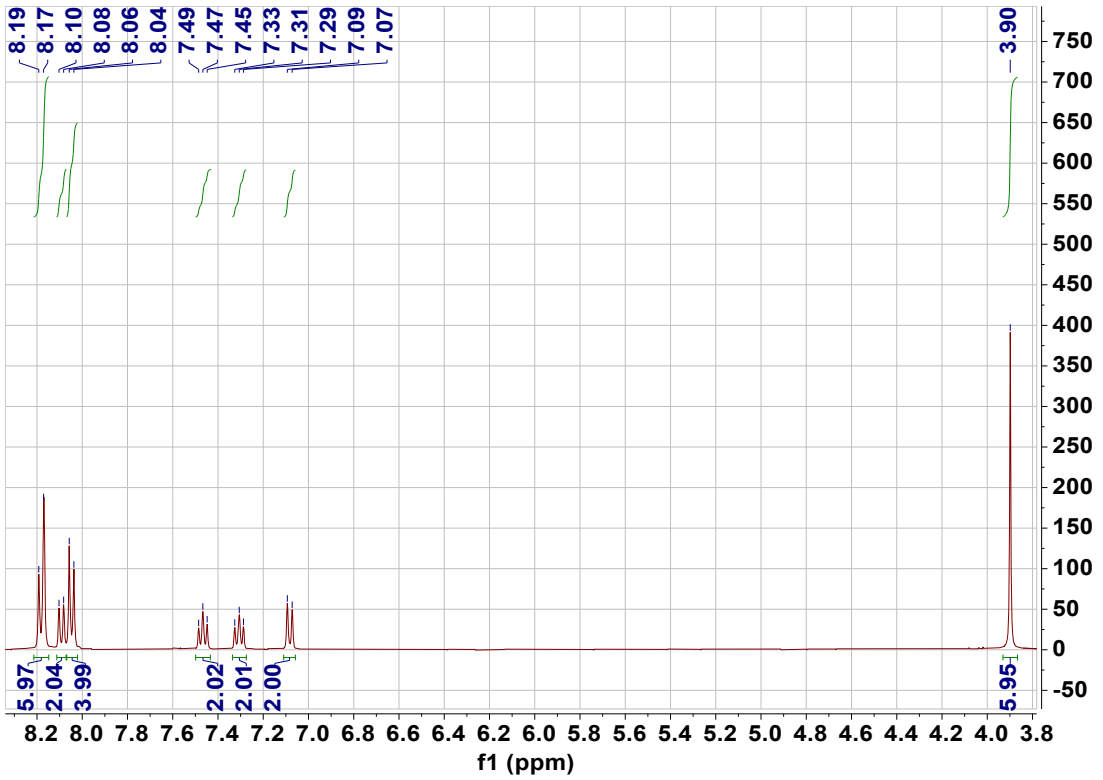
8.19
8.17
8.10
8.08
8.06
8.04
7.49
7.47
7.45
7.33
7.31
7.29
7.09
7.07
3.90
5.97
2.04
3.99
2.02
2.01
2.00
5.95
f1 (ppm)

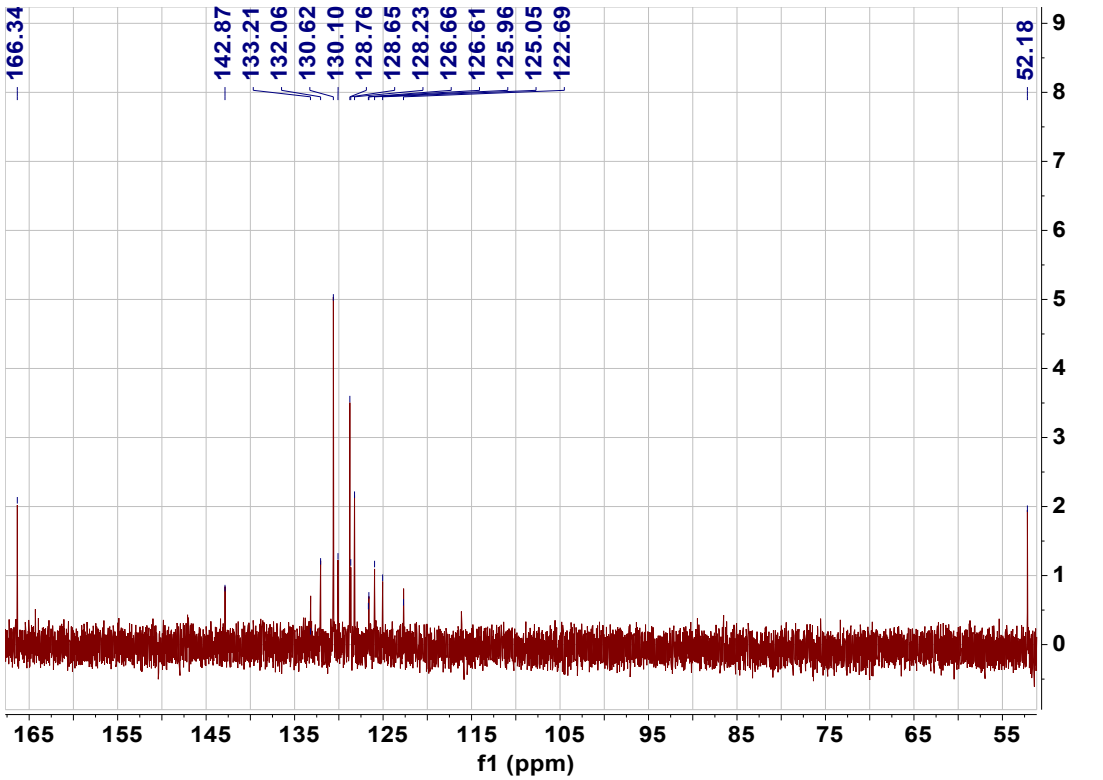
166.34
142.87
133.21
132.06
130.62
130.10
128.76
128.65
128.23
126.66
126.61
125.96
125.05
122.69
52.18
f1 (ppm)

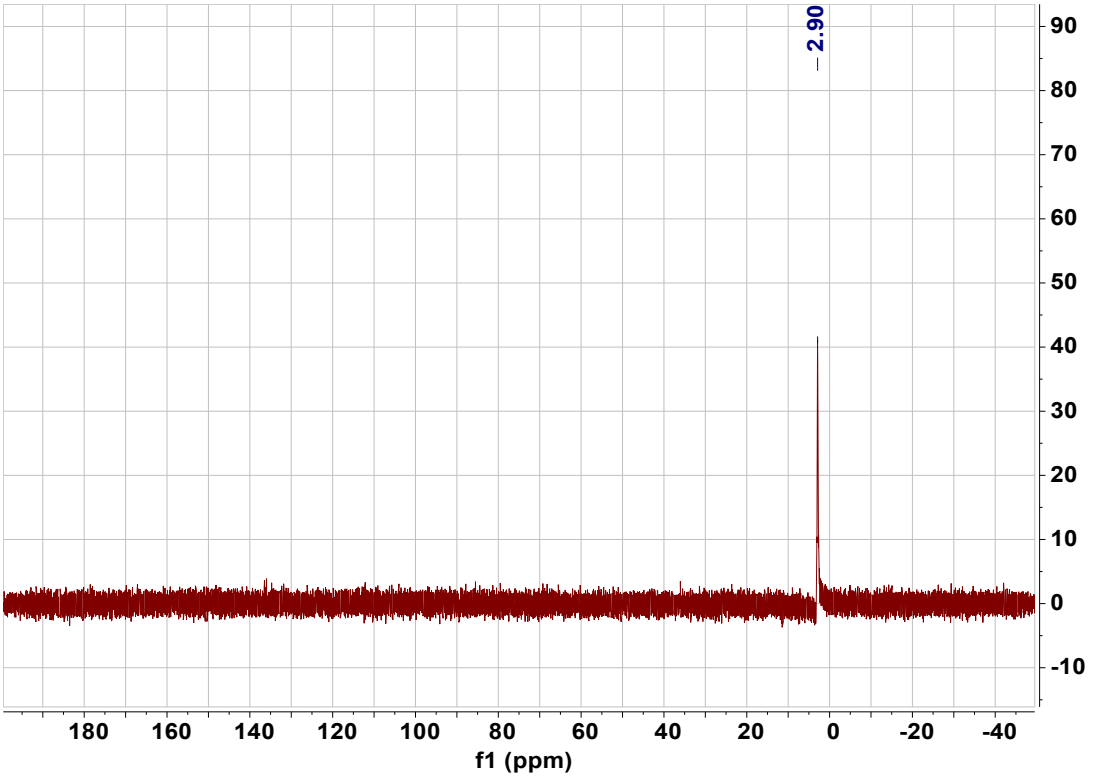


**Figure S9.** $^{1}$H NMR (400 MHz, DMSO-$d_6$), $^{13}$C NMR (101 MHz, DMSO-$d_6$) and $^{31}$P NMR (162 MHz, DMSO-$d_6$) spectra of **5**.

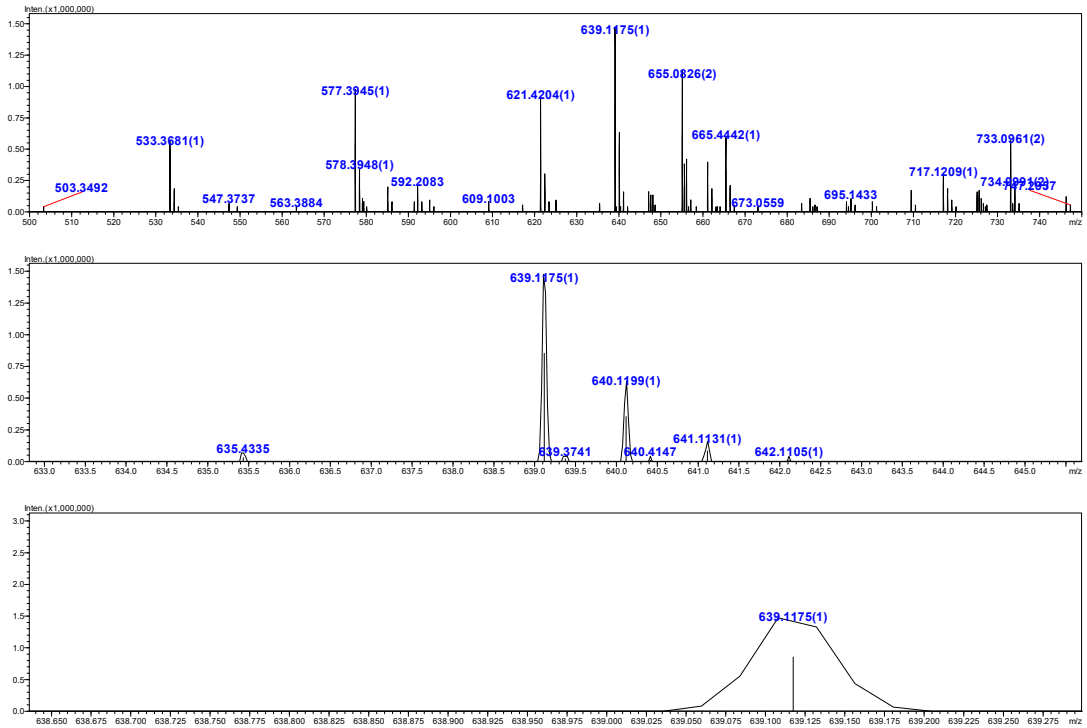


**Figure S10.** HRMS spectra of **5** (ES$^{+}$).

Synthesis of **(*R*)-H$_3$L**

A solution of **5** (0.2 g, 0.32 mmol) in methanol (20 mL), THF (10 mL) and 1M aqueous LiOH (3.2 mL) was heated at 50 °C for 24 h. The solution was cooled to room temperature and acidified to pH ~ 1 with 2 M HCl, extracted with EtOAc (100 mL ×3), dried over $Na_2SO_4$, and concentrated under reduced pressure to give (*R*)-$H_3L$ (0.17 g) as a white solid in 90% yield. $^1$H NMR (400 MHz, DMSO-$d_6$) δ 8.27 (s, 2H), 8.15 (d, $J$ = 8.3 Hz, 2H), 8.05 (d, $J$ = 8.0 Hz, 4H), 7.97 (d, $J$ = 7.8 Hz, 4H), 7.55 (t, $J$ = 7.5 Hz, 2H), 7.42 – 7.34 (m, 2H), 7.18 (d, $J$ = 8.5 Hz, 2H). $^{13}$C NMR (101 MHz, DMSO-$d_6$) δ 167.3, 145.3, 141.7, 132.9, 131.8, 131.3, 130.7, 130.2, 129.8, 129.2, 128.9, 127.2, 126.1, 125.9, 122.4. $^{31}$P NMR (162 MHz, DMSO-$d_6$) δ 1.46. HR-MS (ES$^+$) calculated for $C_{34}H_{22}O_8P^+$ (M+H$^+$) 611.0866, found 611.0866.

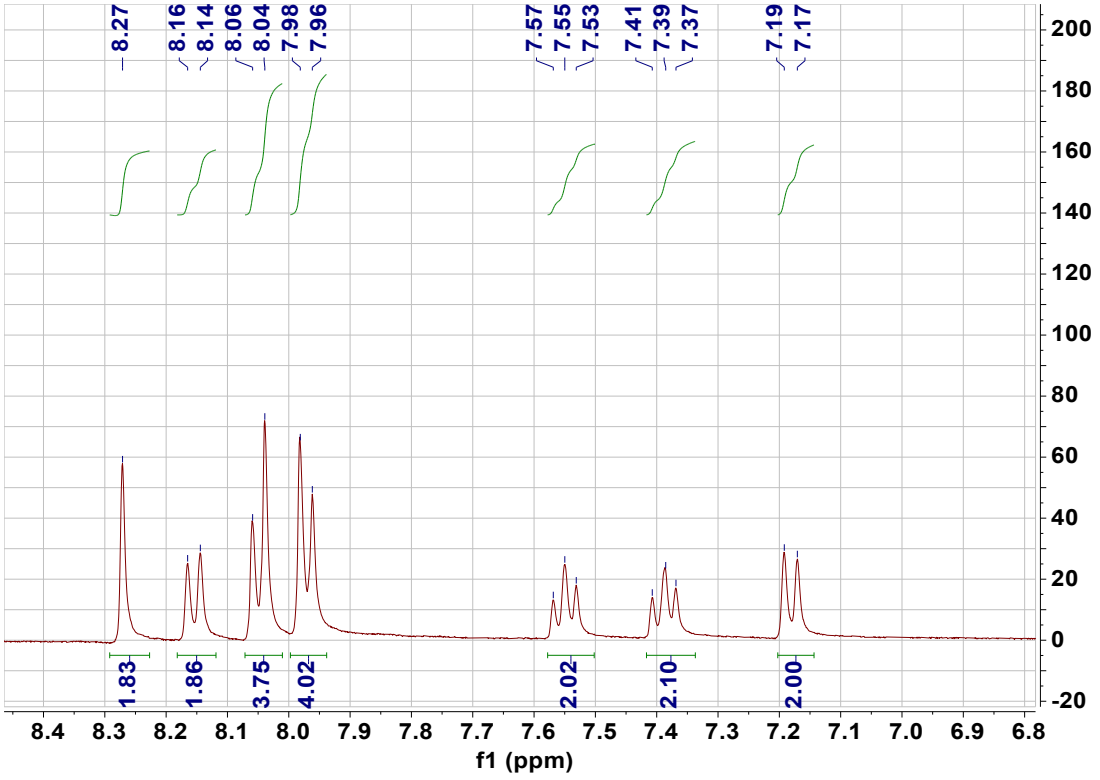

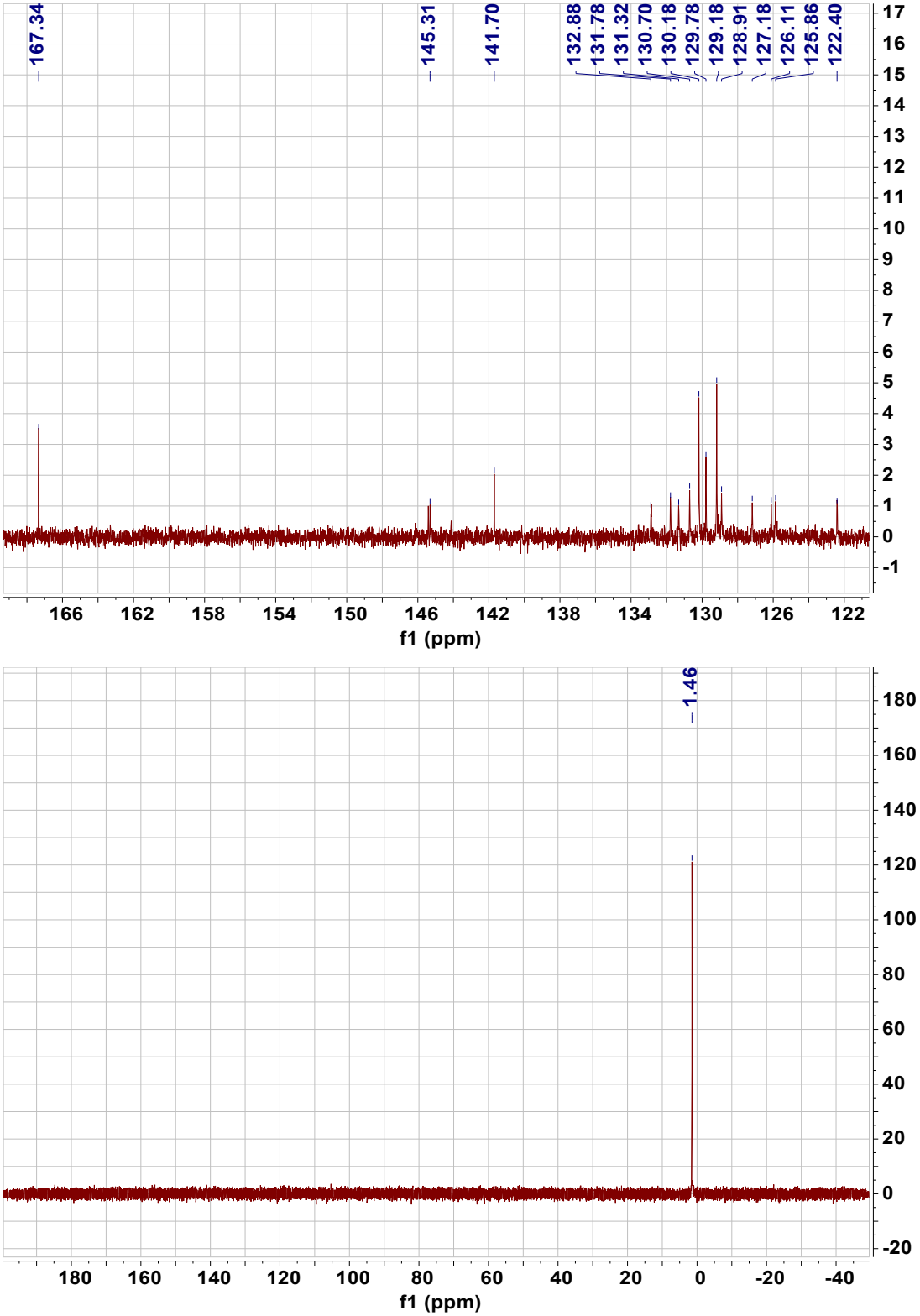


**Figure S11.** $^{1}$H NMR (400 MHz, DMSO-$d_6$), $^{13}$C NMR (101 MHz, DMSO-$d_6$) and $^{31}$P NMR (162 MHz, DMSO-$d_6$) spectra of (*R*)-$H_3$L.

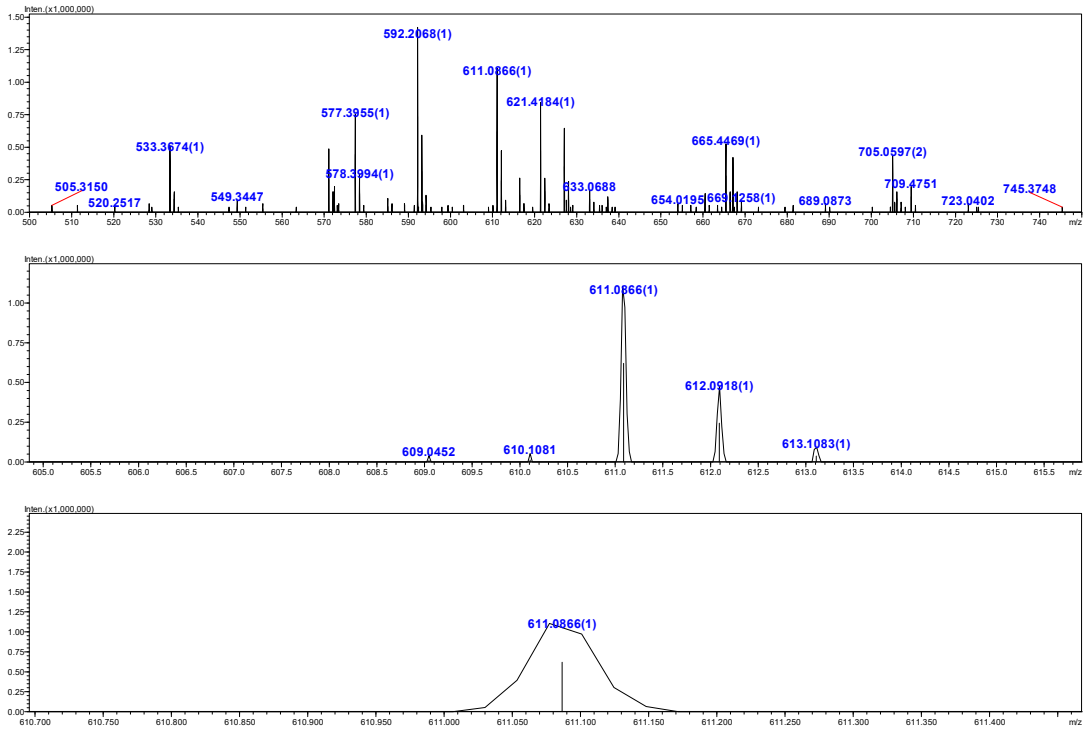


**Figure S12.** HRMS spectra of (*R*)-$H_3L$ ($ES^+$).

## 3. Supplementary Figures and Tables

**Table S1. Gelation Properties of (*R*)-$H_3L$[a]**

| Solvent | Result | Solvent | Result | Solvent | Result |
|---|---|---|---|---|---|
| $H_2O$ | I | $(CH_3CH_2)_2O$ | I | DMSO | S |
| $CHCl_3$ | I | $CH_3COOCH_2CH_3$ | I | THF/$H_2O$ | S |
| $CH_2Cl_2$ | I | THF | S | *i*PrOH/$H_2O$ | S |
| n-Hexane | I | EtOH | S | EtOH/$H_2O$ (1/1, v/v) | G (34 mM) |
| $CH_3CN$ | I | MeOH | S | MeOH/$H_2O$ (1/1, v/v) | G (34 mM) |
| $BrCH_2CH_2Br$ | I | DMF | S | DMF/$H_2O$ (1/1, v/v) | G (28 mM) |
| Acetone | I | Isopropyl alcohol | S | DMSO/$H_2O$ (1/1, v/v) | G (28 mM) |

[a]I: insoluble, G: stable gel, S: sol. In parentheses, critical gelation concentration (CGC) and the volume ratio of organic solvent and water required to form stable water-induced gels, respectively, are given.

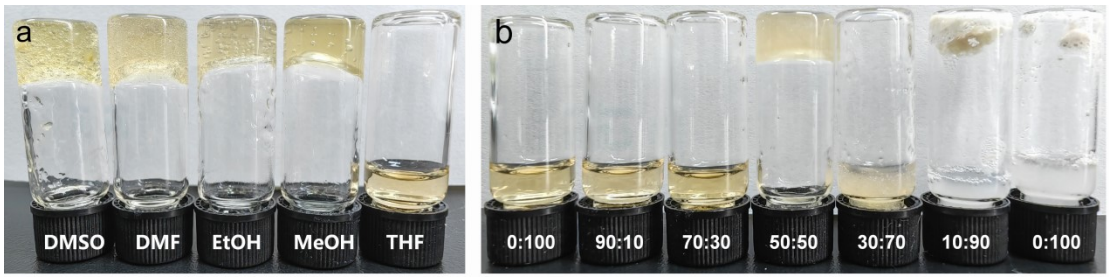

**Figure S13.** (a) The gelation of (*R*)-$H_3L$ in different solvents at respective CGC. (b) The effect of adding water on the gelation of (*R*)-$H_3L$ in EtOH/$H_2O$. From left to right: the ratio of water ($f_w$) was increased from 0 to 100%.

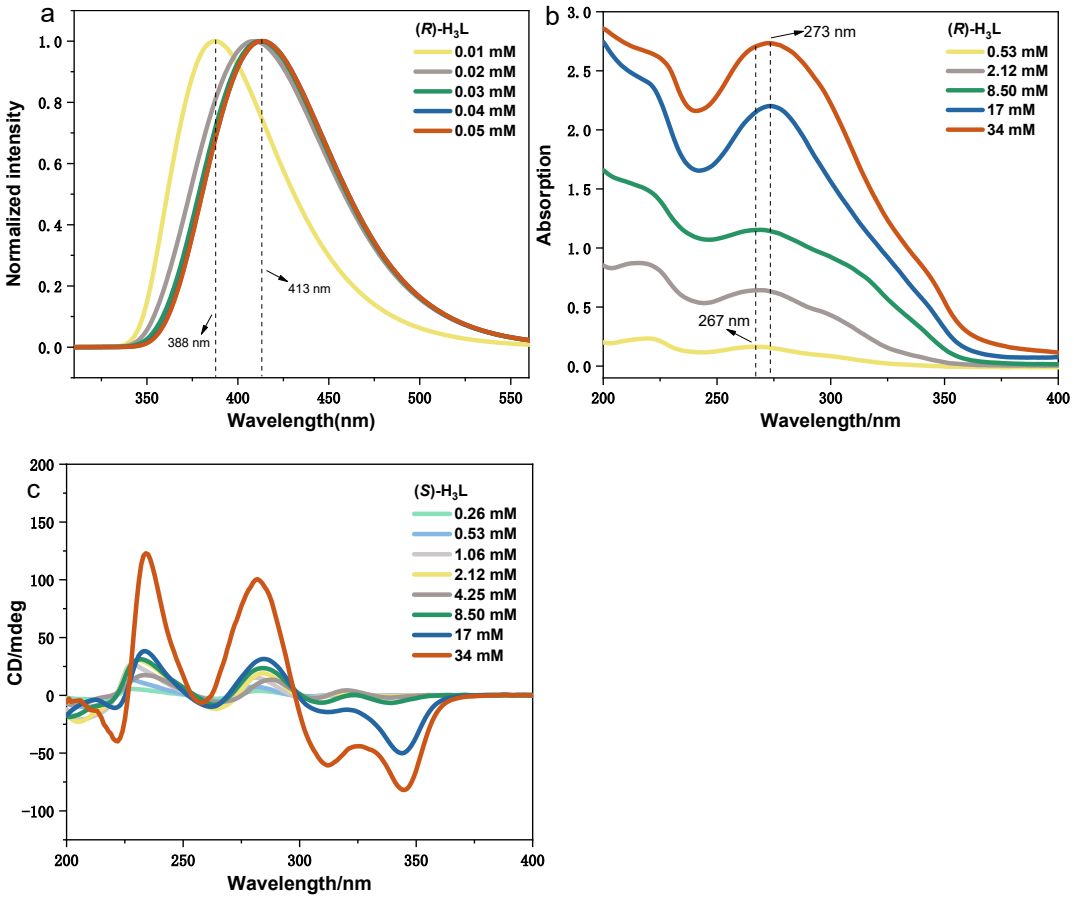


**Figure S14.** (a) Fluorescence and (b) UV spectra of (*R*)-$H_3L$ at different concentrations in EtOH/$H_2O$ (1/1, v/v). For fluorescence: $\lambda_{exc}$ = 290 nm, slits: 5 nm/5 nm. (c) CD spectra of (*S*)-$H_3L$ at different concentrations in EtOH/$H_2O$ (1/1, v/v).

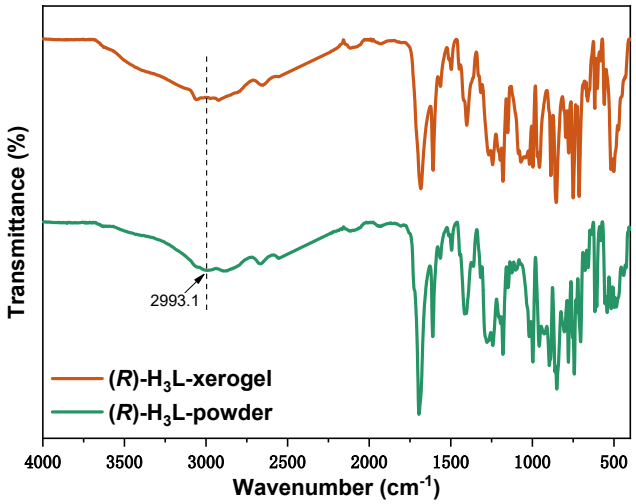

**Figure S15.** FT-IR spectra of (*R*)-$H_3L$ powder and (*R*)-$H_3L$ xerogel.

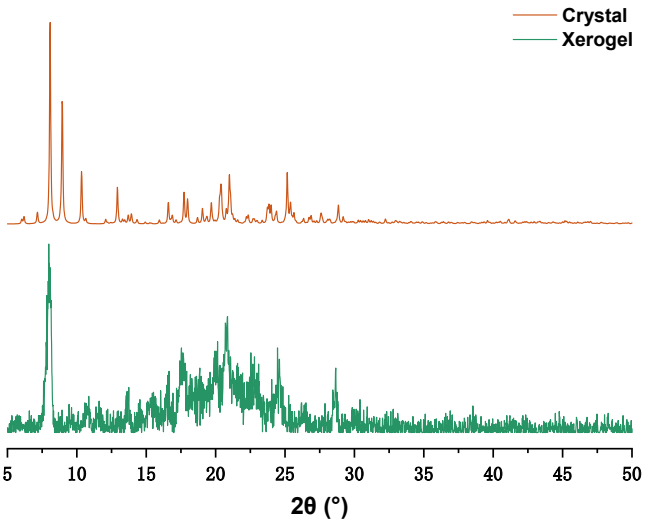


**Figure S16.** PXRD pattern of (*R*)-$H_3L$ xerogel and PXRD pattern simulated from (*R*)-$H_3L$ X-ray crystal data.

**Table S2.** Crystal data and structure refinement for (*R*)-$H_3L$.

| | |
|---|---|
| Empirical formula | $C_{70}H_{56}O_{22}P_2$ |
| Formula weight | 1311.08 |
| Temperature (K) | 302.0 |
| Wavelength (Å) | 0.71073 |
| Crystal system | orthorhombic |
| Space group | $P2_12_12_1$ |
| Unit cell dimensions | a = 13.6884(7) Å, α = 90° |
| | b = 17.0653(10) Å, β = 90° |
| | c = 28.5141(13) Å, γ = 90° |
| Volume (Å$^3$), Z | 6660.8(6), 4 |
| Calculated density (g/cm$^3$) | 1.307 |
| Crystal size (mm$^3$) | 0.18 × 0.11 × 0.11 |
| Absorption coefficient (mm$^{-1}$) | 0.143 |
| *F*(000) | 2728.0 |
| 2θ range for data collection (°) | 3.814 to 55.032 |
| Limiting indices | $-17 \le h \le 17$, $-19 \le k \le 22$, $-37 \le l \le 36$ |
| Reflections collected | 61453 |
| Data / restraints / parameters | 15249/9/862 |
| $R_{int}$ | 0.0899 |
| Refinement method | Full-matrix least-squares on $F^2$ |
| Goodness-of-fit on $F^2$ | 1.016 |
| Final R indices [I>2sigma(I)] | $R_1 = 0.0561$, $wR_2 = 0.1216$ |
| R indices (all data) | $R_1 = 0.1117$, $wR_2 = 0.1480$ |
| Flack parameter | 0.01(5) |
| Largest diff. peak and hole (e.Å$^{-3}$) | 0.41/-0.27 |

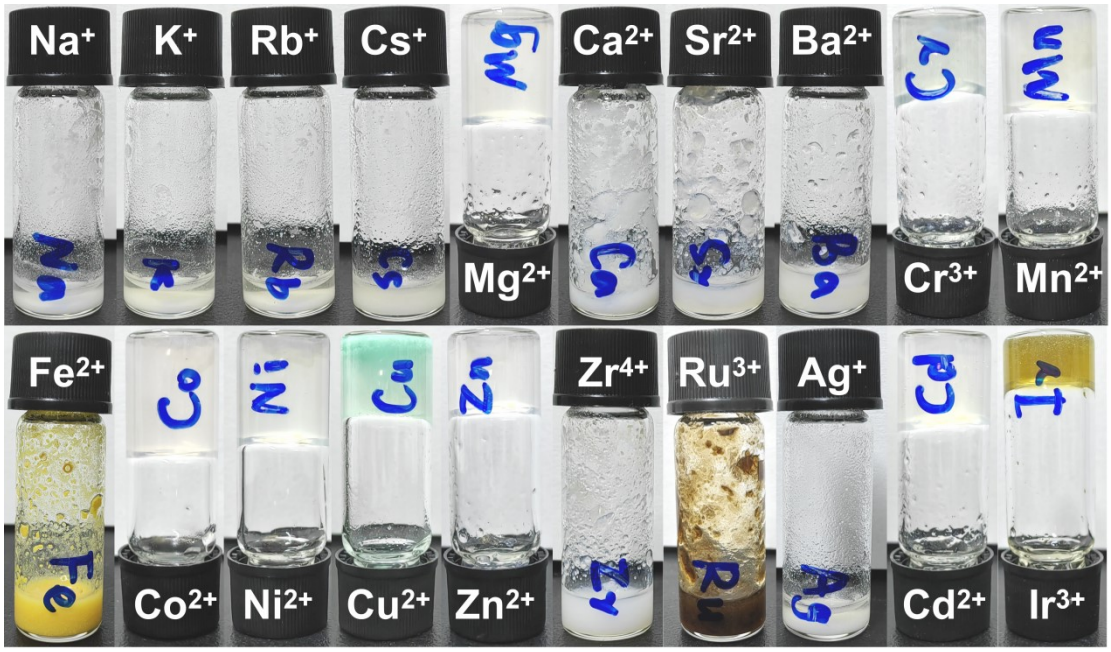


**Figure S17.** The gelation of (*R*)-$H_3L$ (5 mg, 8.5 mmol) coordinated with 1eq various metal ions in EtOH/$H_2O$ (1/1, v/v) at their respective CGC concentrations (for the precipitated sample, the volume of mixed solvent is 200 μL).

**Table S3. Gelation Properties of (*R*)-$H_3L$ coordinated with various metal ions**[a]

| Metal salt | Result | Metal salt | Result |
|---|---|---|---|
| NaCl | P | $FeCl_3·6H_2O$ | P |
| KCl | P | $CoCl_2·6H_2O$ | G（7.72 mM） |
| RbCl | P | $NiCl_2·6H_2O$ | G（8.50 mM） |
| CsCl | P | $CuCl_2·2H_2O$ | G（14.16 mM） |
| $MgCl_2$ | G（8.50 mM） | $ZnCl_2$ | G（10.62 mM） |
| $CaCl_2$ | P | $ZrCl_4$ | P |
| $SrCl_2·6H_2O$ | PG | $RuCl_3·H_2O$ | PG |
| $BaCl_2·2H_2O$ | PG | $AgNO_3$ | P |
| $CrCl_3·6H_2O$ | G（12.14 mM） | $CdCl_2·2.5H_2O$ | G（10.62 mM） |
| $MnCl_2$ | G（9.44 mM） | $IrCl_3·H_2O$ | G（17 mM） |

[a]P: precipitate, G: stable gel, PG: partial gel. In parentheses, critical gelation concentration (CGC) and the volume ratio of organic solvent and water required to form stable water-induced gels, respectively, are given.

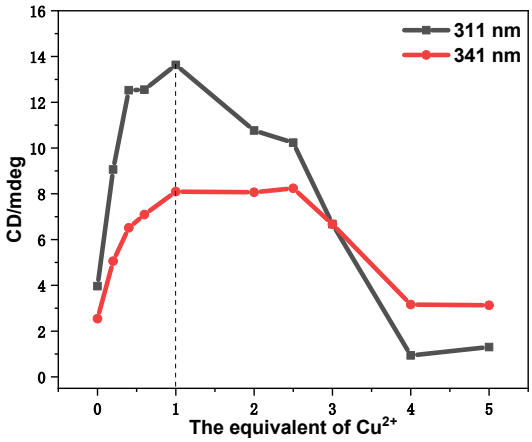


**Figure S18.** CD intensity of (*R*)-$H_3L$ ($1\times10^{-4}$ M) coordinated with various equivalents of $Cu^{2+}$ in EtOH/$H_2O$ (1/9, v/v) at 311 nm and 341 nm.

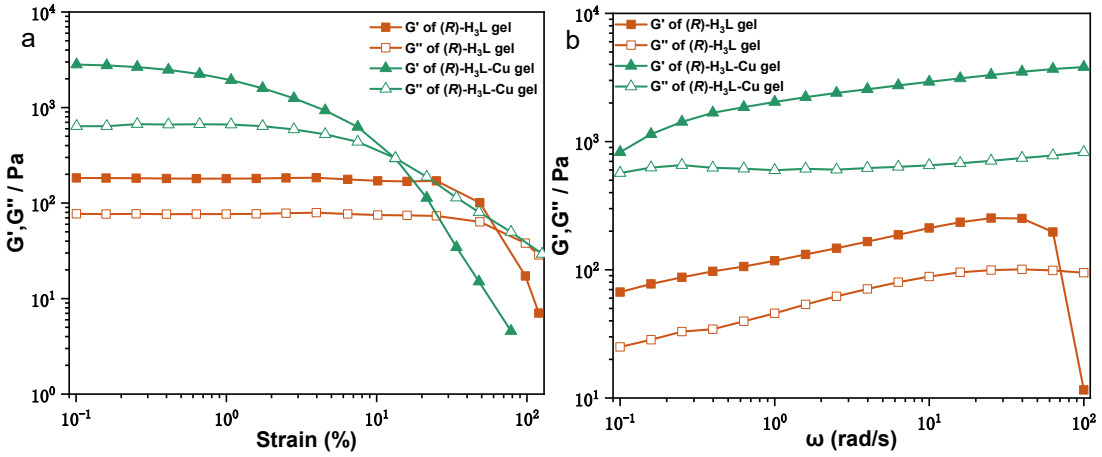


**Figure S19.** (a) Dynamic strain sweep measurements of (*R*)-$H_3L$ gel and (*R*)-$H_3L$-Cu gel (both at 34mM) with a frequency $\omega = 6.28$ rad $s^{-1}$ at 25 ℃ (from 0.1 to 100%). (b) Dynamic frequency sweep measurements of (*R*)-$H_3L$ gel and (*R*)-$H_3L$-Cu gel (both at 34mM) with a strain $\gamma = 0.1\%$ at 25 ℃ (from 0.1 to 100 rad $s^{-1}$).

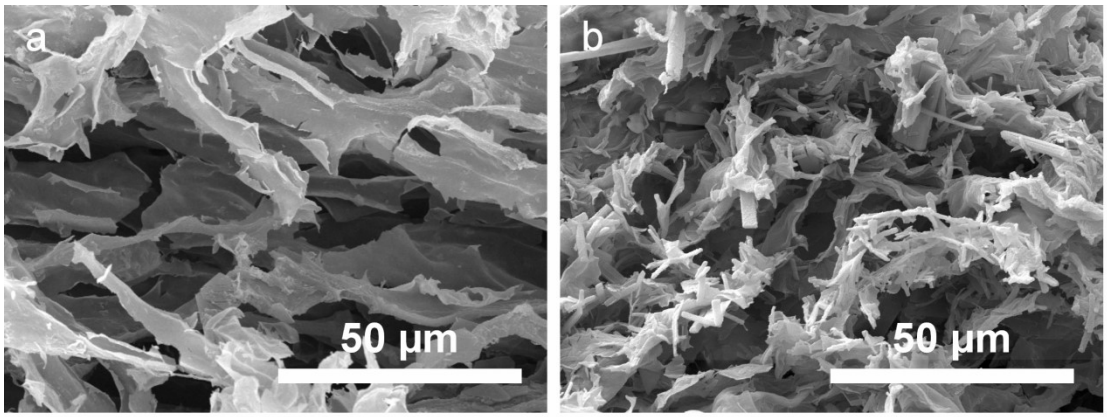


**Figure S20.** SEM image of (a) (*S*)-$H_3L$ xerogel and (b) (*S*)-$H_3L$-Cu xerogel obtained from EtOH/$H_2O$ (1/1, v/v).

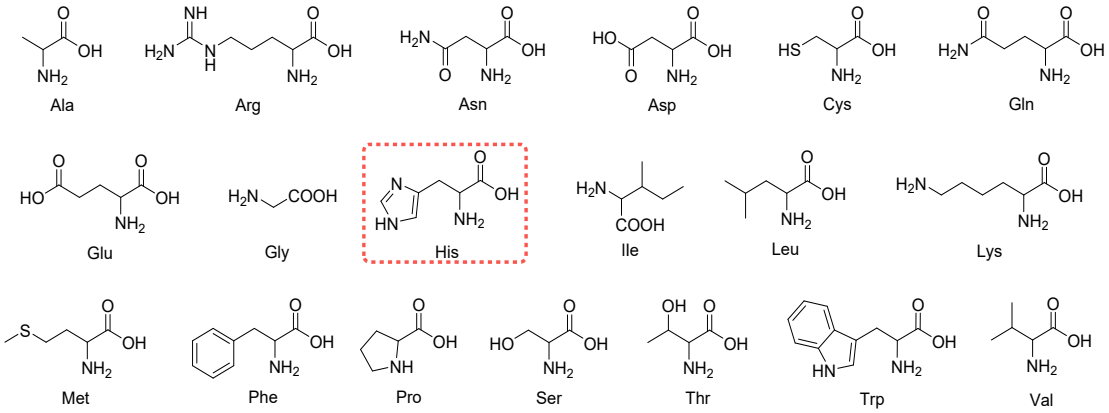


**Scheme S2.** Structures of amino acids used in this study.

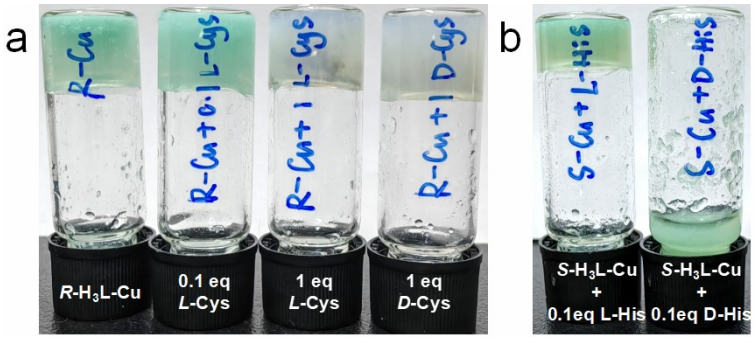


**Figure S21.** (a) (*R*)-$H_3$L-Cu gel in the presence of 1eq *L*- or *D*-Cys. (b) The enantioselective responses of (*S*)-$H_3$L-Cu gel toward 0.01 eq *L*-His (left) and *D*-His (right).